Electrochimica Acta 54 (2009) 7502–7506

Contents lists available at ScienceDirect

Electrochimica Acta

journal homepage: www.elsevier.com/locate/electacta

Electrochemical behavior of Ni(II)/Ni in a hydrophobic amide-type room-temperature ionic liquid

Yan-Li Zhu, Yukari Kozuma, Yasushi Katayama*,[1], Takashi Miura

Department of Applied Chemistry, Faculty of Science and Technology, Keio University, Hiyoshi 3-14-1, Kohoku-ku, Yokohama, Kanagawa 223-8522, Japan

ARTICLE INFO

Article history:
Received 17 June 2009
Received in revised form 31 July 2009
Accepted 31 July 2009
Available online 11 August 2009

Keywords:
Ionic liquid
Nickel
1-Butyl-1-methylpyrrolidinium bis(trifluoromethylsulfonyl)amide
Room-temperature molten salt
Electrodeposition

ABSTRACT

Electrochemical reaction of Ni(II)/Ni was investigated in a hydrophobic room-temperature ionic liquid, 1-butyl-1-methylpyrrolidinium bis(trifluoromethylsulfonyl)amide (BMPTFSA) containing $Ni(TFSA)_2$ as a Ni source. The UV–vis spectra showed that Ni(II) in BMPTFSA is octahedrally coordinated with $TFSA^-$ anions. The average activation energy for the diffusion coefficients of this Ni(II) complex was ~26 kJ mol^{-1}, which was close to that for the viscosity. The diffusion coefficient of Ni(II) was estimated to be 9.3×10^{-8} cm^2 s^{-1}. Chronoamperometric measurements showed that the electrodeposition of Ni on a platinum substrate involved three-dimensional instantaneous nucleation under diffusion control at room-temperature. The electrodeposits obtained by galvanostatic electrolysis with the current density of −0.046 mA cm^{-2} at 70 and 100 °C were identified as metallic Ni by XRD.

1. Introduction

The electrodeposited nickel is mainly used in the corrosion- and wear-resistant coating industry. Recently, Ni or its alloy, such as Ni–Co, Ni–Fe and Ni–W, has been also applied into the production of micro-mechanical devices, fabricating magnetic materials for data storage and magnetic sensors, and catalytic industry, which requires a better control of the morphologies of the deposits [1–6]. It is possible to obtain Ni or its alloy electrochemically from aqueous solutions. However, it is difficult to prevent hydrogen evolution, which leads to the low current efficiency and worse quality of deposits due to the hydrogen embrittlement. Some room-temperature ionic liquids (RTIL) are expected to be the alternative aprotic media for electrodeposition of various metals, since they generally have several distinctive properties, such as the wide potential windows, acceptable conductivity compared to non-aqueous electrolytes and negligible vapor pressure (up to 300 °C) [7,8].

The electrodeposition of Ni has been mainly studied in acidic chloroaluminate or chlorozincate ionic liquids [9–18] except the choline chloride–urea eutectic [19] and the DCA^--based (DCA^-: dicyanamide) ionic liquids [20]. In case of chloroaluminate or chlorozincate ionic liquids, codeposition of Al or Zn makes it difficult to obtain Ni alloys containing the metals less noble than Al or Zn. Thus, the ionic liquids containing no metal species are promising for electrodeposition of Ni alloys containing various metals. Bis(trifluoromethylsulfonyl)amide ($TFSA^-$)-based ionic liquids are expected to be preferable for electrodeposition of various metals including Ni since these ionic liquids are stable against moisture and immiscible with water.

Among the $TFSA^-$-based ionic liquids, the system containing 1-butyl-1-methylpyrrolidinium (BMP^+) received much attention because of its low melting point and high cathodic stability [8,21]. From this electrolyte, some metals have been electrodeposited successfully. Dense and adherent deposit of aluminum is an example [22,23]. The grain size of the deposit in the nanometer regime was smaller than those obtained from EMIMTFSA ($EMIM^+$: 1-ethyl-3-methylimidazolium), which was in the micrometer range. Bebensee et al. also obtained the nanocrystalline aluminum from the same ionic liquid [24]. Some other deposits, such as semiconductor silicon [25,26], transition metals of tantalum and copper, selenium and indium [27–29] were obtained from this kind of ionic liquid. The electrodeposit of amorphous manganese on tungsten, nickel, or copper foils was identified by the energy-dispersive spectrometer [30,31]. The current efficiency was higher than 97% regardless of the applied potential. However, the electrodeposition of Ni has not been reported in this ionic liquid. In the present study, the electrochemical reaction of Ni(II)/Ni was investigated in 1-butyl-1-methylpyrrolidinium bis(trifluoromethylsulfonyl)amide (BMPTFSA) at various temperatures.

* Corresponding author. Tel.: +81 45 566 1561; fax: +81 45 566 1561.
E-mail address: katayama@applc.keio.ac.jp (Y. Katayama).
[1] ISE member.

0013-4686/$ – see front matter © 2009 Elsevier Ltd. All rights reserved.
doi:10.1016/j.electacta.2009.07.088

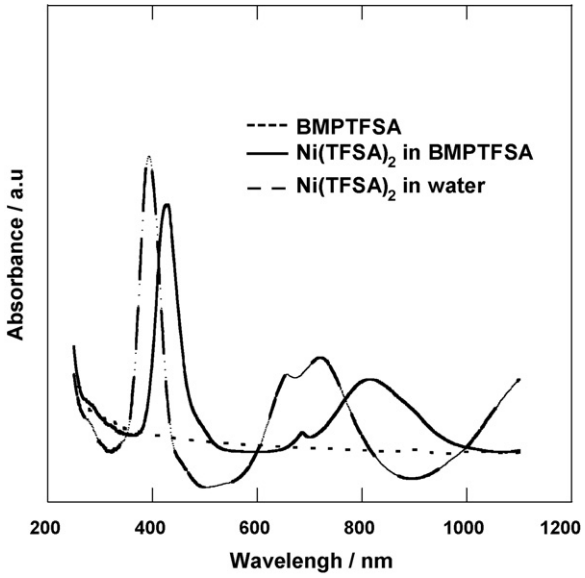

Fig. 1. UV–vis spectra of 0.1 M $Ni(TFSA)_2$/BMPTFSA and $Ni(TFSA)_2/H_2O$.

2. Experimental

BMPBr was prepared by the reaction of 1-methylpyrrolidine (Tokyo Kasei, >95%) and butylbromide (Tokyo Kasei, >98%) in dehydrated acetonitrile (Junsei Chemical, 99.5%) at room-temperature, then purified by recrystallization and finally dried under vacuum at 120 °C for 24 h. BMPTFSA was obtained by reaction of BMPBr with LiTFSA (Kanto Kagaku, >99.98%) in deionized water, separated by extracting into dichloromethane (Junsei Chemical, 99.0%), and then finally dried under vacuum at 120 °C for 24 h. The water content in BMPTFSA was below 10 ppm, which was determined by Karl Fischer titration (Metrohm, 831 KF Coulometer). $Ni(TFSA)_2$ was prepared by reacting $NiCO_3{\cdot}Ni(OH)_2{\cdot}4H_2O$ (Kanto Chemical) with HTFSA (Morita Kagaku, >99%) at 80 °C under agitation, filtrated to eliminate the unreacted inorganic metal salts, and then dried under vacuum at 160 °C for 24 h [32]. The product was yellow solid powder. The yellow electrolyte was obtained by dissolving a certain amount of $Ni(TFSA)_2$ into BMPTFSA.

A three-electrode cell was used for all the electrochemical measurements and electrodeposition experiments with the aid of a potentiostat/galvanostat (Hokuto Denko, HABF-501). For the electrochemical measurements, a platinum disk electrode (7.85×10^{-3} cm^2) was employed as a working electrode after mirror polishing. Platinum wire was used as a counter electrode. Silver wire immersed in BMPTFSA containing 0.1 mol dm^{-3} $AgCF_3SO_3$ (Aldrich, >99.0%) was used as a reference electrode, which was separated from main electrolyte by porous Vycol glass. All the potentials in this paper were referred to this Ag/Ag(I) electrode. For the electrodeposition experiments, a copper disk electrode (7.06×10^{-2} cm^2) was used as a substrate after mirror polishing, electrolytic degreasing in alkali solution and washing with 10 vol% H_2SO_4 and distilled water. Ni (Nilaco) wire was employed as a counter electrode. The reference electrode was as the same as described above.

Handling of all the hygroscopic reagents and electrochemical experiments were performed in an argon-filled glove box with a continuous gas purification apparatus (Miwa Seisakujyo Co. Ltd., DB0-1K-SH). The concentrations of H_2O and O_2 in the gas were kept under 0.8 and 1 ppm, respectively.

The absorption spectra of BMPTFSA containing $Ni(TFSA)_2$ was measured by using an air-tight quartz cell (light path length 0.1 cm) with the aid of UV–vis spectrometer (JASCO, V-530). The electrodeposits washed with ethanol (Wako, >99.8%) and dried in the air were characterized by a scanning electron microscope (SEM, KEYENCE VE-9800), X-ray diffractometer (XRD, Rigaku RAD-C, Cu Kα), X-ray photoelectron spectrometer (XPS, JOEL JPPS-9000 MC) and energy-dispersive X-ray analysis (EDX, EDAX Phoenix).

3. Results and discussion

3.1. Solvation structure of Ni(II) in BMPTFSA

The coordination chemistry is an important factor for the electrochemical behavior of metal ions in ionic liquids. Gale et al. [12] has reported that reduction of Ni(II) species is possible in acidic chloroaluminate ionic liquids while divalent Ni cations are likely to form a chlorocomplex, $[NiCl_4]^{2-}$, in basic ionic liquids, and the complex cannot be reduced to Ni within the electrochemical potential window. Fig. 1 shows the absorption spectra of 0.1 M $Ni(TFSA)_2$/BMPTFSA and $Ni(TFSA)_2/H_2O$ at room temperature. The assignments of the absorption bands are summarized in Table 1. The maximum absorption wavelength (λ_{max} = 429) and molar absorption coefficient (ε = 18) of 0.1 M $Ni(TFSA)_2$ in BMPTFSA were close to those in water, suggesting the divalent Ni cations are octahedrally coordinated by six oxygen atoms of $TFSA^-$ anions, as reported in $Ni(TFSA)_2$/EMITFSA (EMI^+: 1-ethyl-3-methylimidazolium) [33]. Thus, the dissolved Ni species is considered as some anionic complexes like $[Ni(TFSA)_3]^-$.

3.2. Cyclic voltammetry

Fig. 2 shows the cyclic voltammograms of a Pt electrode in 0.1 M $Ni(TFSA)_2$/BMPTFSA with various scan rates at room-temperature (25 °C). A cathodic and anodic current peak were observed at about −1.7 and +0.6 V, respectively. The cathodic and anodic peaks only appeared in the presence of Ni(II). Moreover, the deposit obtained by the potentiostatic cathodic reduction at −1.9 V was confirmed as metallic Ni by XPS and EDX. Thus, the cathodic peak was ascribed to the reduction of Ni(II) to Ni(0) while the anodic current peak was assignable to the anodic dissolution of the Ni deposited during the preceding cathodic scan. Since the cathodic peak potential shifted to more negative side with increasing the scan rates and the peak separation exceeded 2.0 V, the electrode reaction of Ni(II)/Ni in BMPTFSA was regarded as electrochemically irreversible. As seen in Fig. 2, the integrated electric charges of the oxidation peak were smaller than those of the reduction ones, suggesting the electrodeposited Ni during the cathodic scan could not be stripped completely during the anodic scan, probably because the concentration of Ni(II) near the electrode increased up to its saturated concentration quickly resulting in the hindrance of the anodic dissolution. The similar behavior was also known for the cyclic voltammetry of Mn [30] and Co [35] in BMPTFSA.

Table 1
UV–vis spectra data (λ: nm, ε: mol^{-1} dm^3 cm^{-1}).

$Ni(TFSA)_2$ in BMPTFSA	$Ni(TFSA)_2$ in H_2O [34]	$NiCl_2$ in basic chloroaluminate ionic liquid [12]	Assignment [34]
429 nm (ε = 18)	395 nm (ε = 5.2)	705 nm (ε = 175)	$^3T_{1g} \leftarrow {}^3A_{2g}$
815 nm (ε = 7.4)	724 nm (ε = 2.1)	658 nm (ε = 169)	$^3T_{1g} \leftarrow {}^3A_{2g}$
686 nm (ε = 4.2)	658 nm (ε = 2.0)	-	$^1E_g \leftarrow {}^3A_{2g}$

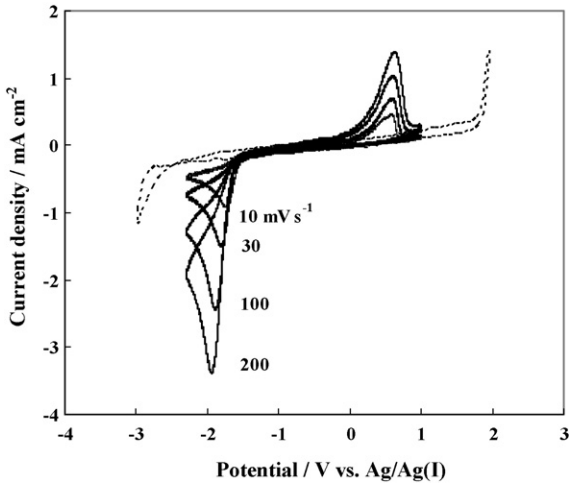

Fig. 2. Cyclic voltammograms of a Pt electrode in 0.1 M $Ni(TFSA)_2$/BMPTFSA with various scan rates at room-temperature. The dotted curve shows the cyclic voltammogram in neat BMPTFSA.

Fig. 3 shows the cyclic voltammograms of a Pt electrode in 0.1 M $Ni(TFSA)_2$/BMPTFSA at various temperatures up to 150 °C. The potential of the cathodic peak shifted to the more positive side and the separation between the cathodic and anodic peaks became smaller with elevating temperature, indicating that the overpotential for electrodeposition of Ni in BMPTFSA decreased at higher temperature. This is not surprising because at higher temperature the charge transfer and mobility of the electroactive species will increase while the nucleation overpotential will be decrease [29].

3.3. Electrodeposition of Ni

Electrodeposition of Ni on a copper substrate in 0.1 M $Ni(TFSA)_2$/BMPTFSA at 50, 70 and 100 °C was performed by galvanostatic electrolysis with a current density of $-0.046\,mA\,cm^{-2}$. A black deposit obtained at 50 °C was confirmed as nickel by XPS, but gave no XRD peak assignable to Ni probably due to the small grain size, as shown in Fig. 4. From the image of the deposit in Fig. 5, there were a few cracks. The fine cracks were also found during the electrodeposition of tantalum in BMPTFSA even at 200 °C [27]. On the other hand, the deposits obtained at 70 and 100 °C were

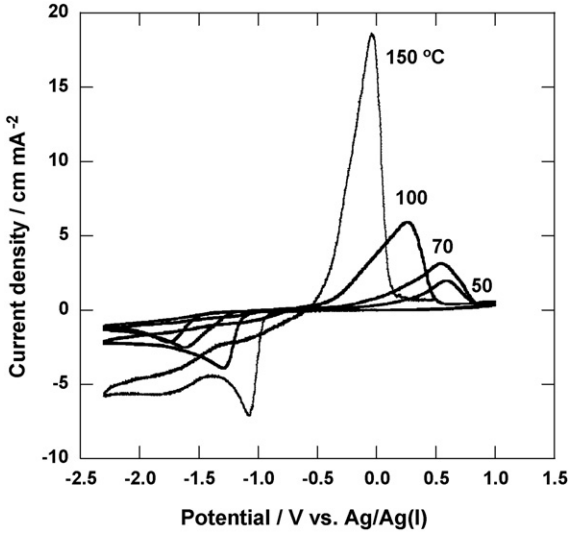

Fig. 3. Cyclic voltammograms of a Pt electrode in 0.1 M $Ni(TFSA)_2$/BMPTFSA at various temperatures (scan rate: $30\,mV\,s^{-1}$).

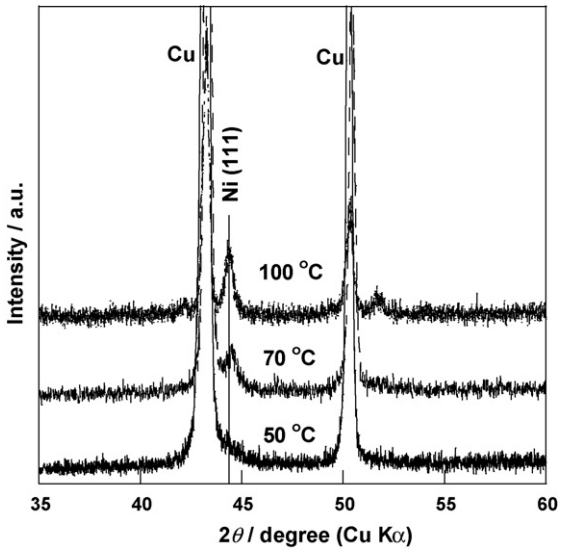

Fig. 4. XRD patterns of electrodeposited Ni films on copper substrates in 0.1 M $Ni(TFSA)_2$/BMPTFSA by galvanostatic electrolysis with a current density of $-0.046\,mA\,cm^{-2}$ (electric charge: $3.6\,C\,cm^{-2}$).

bright, and identified as metallic Ni by XRD, as shown in Fig. 4. The width of the diffraction peaks slightly decreased with an increase in temperature, indicating that the grain size of the deposit became bigger at higher temperature. According to the Scherrer equation, the average grain sizes were about 10 and 15 nm at 70 and 100 °C,

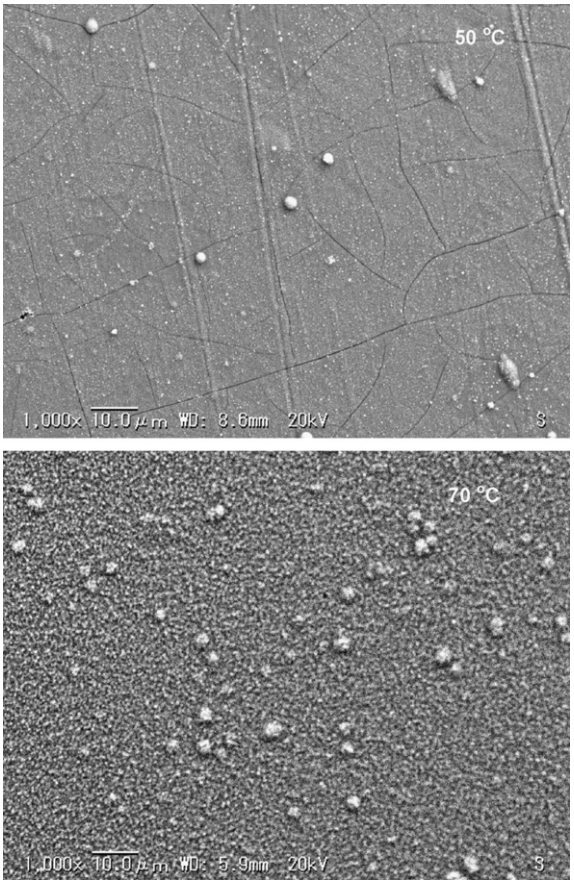

Fig. 5. SEM image of the deposit on a Cu substrate by the galvanostatic electrodeposition in 0.1 M Ni(II)/BMPTFSA at 50 and 70 °C. The current density was $-0.046\,mA\,cm^{-2}$.

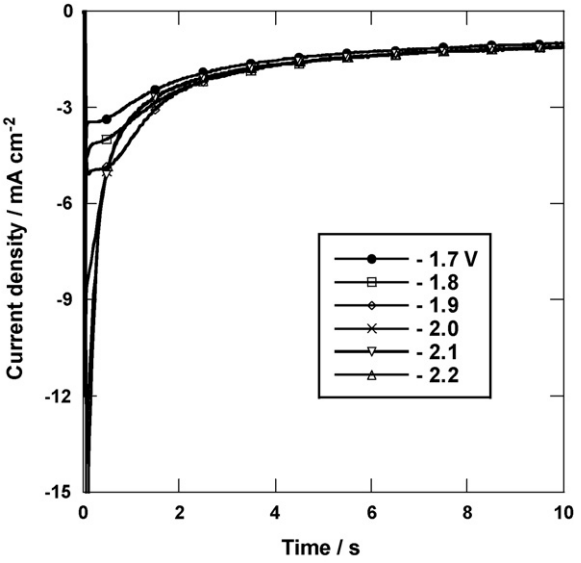

Fig. 6. Chronoamperograms of a Pt electrode in 0.1 M $Ni(TFSA)_2$/BMPTFSA at 25 °C.

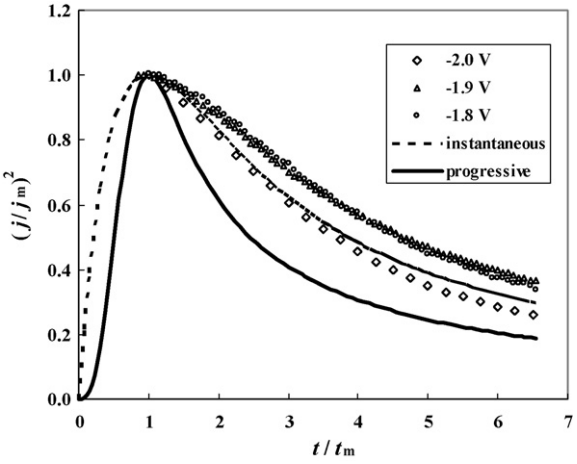

Fig. 8. Dimensionless plots of $(j/j_m)^2$ vs. t/t_m using the data of Fig. 6 (instantaneous (- - -), progressive (—)).

respectively. These values were smaller than those of the electrodeposited Ni obtained from imidazolium-based ionic liquid (about 30–40 nm at room-temperature) [20]. A possible explanation for this difference may be that the pyrrolidinium cations are adsorbed on the Ni deposit, acting as a grain refiner during metal electrodeposition [22].

3.4. The diffusion coefficient of Ni(II) and nucleation/growth of Ni deposit

Fig. 6 shows the chronoamperograms of a Pt electrode in BMPTFSA containing 0.1 M Ni(II). Current peaks characteristic of nucleation process were observed after the charging of the electric double layer. After the peaks, the current densities converged with the elapse of time, indicating that the reduction of Ni(II) is satisfied the Cottrell's criteria and can be regarded as the diffusion-limited process. According to the Cottrell's equation for semi-infinite one-dimensional diffusion [36], the diffusion coefficient of Ni(II) was estimated to be 9.3×10^{-8} cm^2 s^{-1}. From the chronopotentiograms shown in Fig. 7, the diffusion coefficient of Ni(II) was estimated to be 7.5×10^{-8} cm^2 s^{-1} according to the Sand's equation [36], which was close to that from chronoamperometry. The values are smaller than those reported in chloroaluminate ionic liquid (2.8×10^{-6} [37] and 2.1×10^{-7} cm^2 s^{-1} [15]), since the viscosity of the BMPTFSA is higher than those of the chloroaluminate ionic liquids. However, the diffusion coefficient of Ni(II) is close to those of Co(II), Fe(II) and Sn(II) in BMPTFSA [33,38,39].

As shown in Fig. 6, characteristic current peaks were observed after the initial charging current for each step. By fitting those current transient data to the Shaifker nucleation and growth model [40], the relationship between the non-dimensional parameters, $(j/j_m)^2$ and t/t_m, where j_m is the peak current density, t the time and t_m is the time at j_m, was shown in Fig. 8. Compared to the theoretical model, the experimental plots can be explained better by an instantaneous nucleation rather than progressive, suggesting that the initial stage of Ni deposition on a Pt electrode can be regarded as the instantaneous nucleation under diffusion control.

Fig. 9 shows the diffusion coefficients and viscosities of 0.1 M $Ni(TFSA)_2$/BMPTFSA at various temperatures. The diffusion coefficient increased with elevating temperature, obeying the Arrhenius' law. The activation energy for the diffusion coefficients of 0.1 M Ni(II) in BMPTFSA was 26 kJ mol^{-1}, which is close to those for the iron complexes in BMPTFSA (19–29 kJ mol^{-1}) [41]. According to

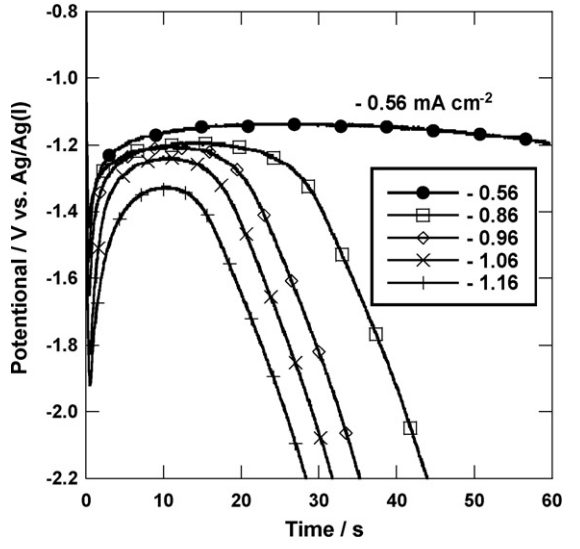

Fig. 7. Chronopotentiograms of a Pt electrode in 0.1 M $Ni(TFSA)_2$/BMPTFSA at 25 °C.

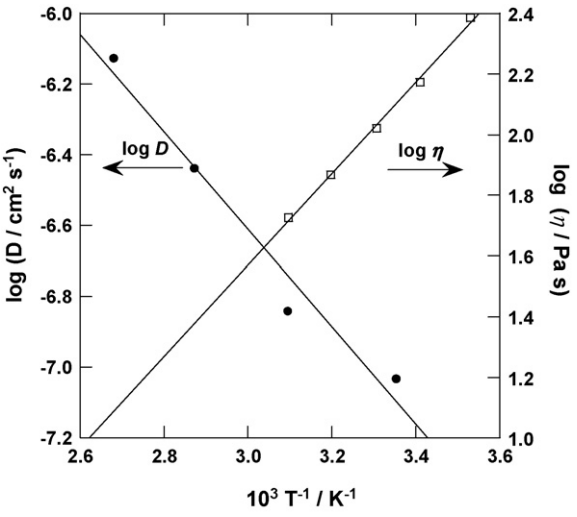

Fig. 9. Dependence of the logarithm of the diffusion coefficient and the viscosity of 0.1 M $Ni(TFSA)_2$/BMPTFSA on the reciprocal of temperature.

the Andrade's formula ($\eta = A\exp(E_a/RT)$, A: constant), the viscosities decreased with elevating temperature. The viscosities of BMPTFSA containing 0.1 M Ni(II) can be fitted to the Andrade's formula and the activation energy was estimated to be 29 kJ mol^{-1}, which is consistent with that for diffusion coefficients.

4. Conclusions

The divalent Ni, presumably existing as [Ni(TFSA)$_3^-$], can be reduced to metallic Ni in a hydrophobic room-temperature ionic liquid, BMPTFSA. The diffusion coefficients of Ni(II) from chronoamperometric and chronopotentiometric techniques were smaller than those reported in chloroaluminate ionic liquid probably due to the higher viscosity of the BMPTFSA. Chronoamperometric experiments showed that the initial stage of the electrodeposition of Ni on a Pt electrode surface involved 3D instantaneous nucleation/growth under diffusion control. The results revealed in this study indicate that the BMPTFSA ionic liquid can be a promising electrolyte for the electrodeposition of various Ni alloys.

Acknowledgments

The present work was financially supported by Grant-in-Aid for Scientific Research on Priority Areas of "Science of Ionic Liquids" (No. 17073016) from the Ministry of Education, Culture, Sports, Science, and Technology, Japan (MEXT).

References

[1] A. Lachenwitzer, S. Morin, O.M. Magnussen, R.J. Behm, Phys. Chem. Chem. Phys. 3 (2001) 3351.
[2] S. Sam, G. Fortas, A. Guittoum, N. Gabouze, S. Djebbar, Sur. Sci. 601 (2007) 4270.
[3] J.Y. Park, M.G. Allen, J. Micromech. Microeng. 8 (1998) 307.
[4] J.L. McCrea, G. Palumbo, G.D. Hibbard, U. Erb, Rev. Adv. Mater. Sci. 5 (2003) 252.
[5] H. Alimadadietal, Mater. Des. 30 (2009) 1356.
[6] D.B. Lee, J.H. Ko, S.C. Kwon, Mater. Sci. Eng. A 380 (2004) 73.
[7] A.P. Abbott, K.J. McKenzie, Phys. Chem. Chem. Phys. 8 (2006) 4265.
[8] Y. Katayama, R. Fukui, T. Miura, J. Electrochem. Soc. 154 (2007) D534.
[9] C.A. Zell, W. Freyland, Chem. Phys. Lett. 337 (2001) 293.
[10] S.P. Gou, I.W. Sun, Electrochim. Acta 53 (2008) 2538.
[11] O. Mannetal, G.B. Pan, W. Freyland, Electrochim. Acta 54 (2009) 2487.
[12] R.J. Gale, B. Gilbert, R.A. Osteryoung, Inorg. Chem. 18 (1979) 2723.
[13] R.P. William, C.L. Hussey, J. Electrochem. Soc. 143 (1996) 130.
[14] T.P. Moffat, J. Electrochem. Soc. 141 (1994) 3059.
[15] O. Mann, W. Freyland, J. Phys. Chem. C 111 (2007) 9832.
[16] M.R. Ali, A. Nishikata, T. Tsuru, J. Electroanal. Chem. 513 (2001) 111.
[17] W. Freyland, C.A. Zell, S.Z.E. Abedin, Electrochim. Acta 48 (2003) 3053.
[18] T.C. Richard, J. Electrochem. Soc. 145 (1998) 1598.
[19] A.P. Abbott, K.E. Ttaib, K.S. Ryder, E.L. Smith, Trans. Inst. Met. Finish. 86 (2008) 234.
[20] M.J. Deng, I.W. Sun, P.Y. Chen, J.K. Chang, W.T. Tsai, Electrochim. Acta 53 (2008) 5812.
[21] D.R. MacFarlane, J. Sun, J. Golding, P. Meakin, M. Forsyth, Electrochim. Acta 45 (2000) 1271.
[22] S.Z.E. Abedin, E.M. Moustafa, R. Hempelmann, H. Natter, F. Endres, Chem. Phys. Chem. 7 (2006) 1535.
[23] S.Z.E. Abedin, E.M. Moustafa, R. Hempelmann, H. Natter, F. Endres, Electrochem. Commun. 7 (2005) 1111.
[24] F. Bebensee, L. Klarhofer, W. Maus-Friedrichs, F. Endres, Sur. Sci. 601 (2007) 3769.
[25] N. Borisenko, S.Z.E. Abedin, F. Endres, J. Phys. Chem. B 110 (2006) 6250.
[26] S.Z.E. Abedin, N. Borisenko, F. Endres, Electrochem. Commun. 6 (2004) 510.
[27] S.Z.E. Abedin, U.W. Biermann, F. Endres, Electrochem. Commun. 7 (2005) 941.
[28] S.Z.E. Abedin, H.K. Farag, E.M. Moustafa, U. Welz-Biermanny, F. Endres, Phys. Chem. Chem. Phys. 7 (2005) 2333.
[29] S.Z.E. Abedin, A.Y. Saad, H.K. Farag, N. Borisenko, Q.X. Liu, F. Endres, Electrochim. Acta 52 (2007) 2746.
[30] M.J. Deng, P.Y. Chen, I.W. Sun, Electrochim. Acta 53 (2007) 1931.
[31] J.K. Chang, C.H. Huang, W.T. Tsai, M.J. Deng, I.W. Sun, P.Y. Chen, Electrochim. Acta 53 (2008) 4447.
[32] T. Katase, T. Onishi, S. Imashuku, K. Murase, T. Hirato, Y. Awakura, Electrochemistry 73 (2005) 686.
[33] K. Fujii, T. Nonaka, Y. Akimoto, Y. Umebayashi, S. Ishiguro, Anal. Sci. 24 (2008) 1377.
[34] B.N. Figgis, Introduction to Ligand Fields, Interscience, 1966.
[35] R. Fukui, Y. Katayama, T. Miura, Electrochemistry 73 (2005) 567.
[36] A.J. Bard, L.R. Faulkner, Electrochemical Methods Fundamentals and Applications, 2nd ed., John Wiley & Sons, Inc., New York, 2001.
[37] W.R. Pitner, C.L. Hussey, G.R. Stafford, J. Electrochem. Soc. 143 (1996) 130.
[38] M. Yamagata, N. Tachikawa, Y. Katayama, T. Miura, Electrochemistry 73 (2005) 564.
[39] N. Tachikawa, N. Serizawa, Y. Katayama, T. Miura, Electrochim. Acta 53 (2008) 6530.
[40] B. Scharifker, G. Hills, Electrochim. Acta 28 (1983) 879.
[41] N. Tachikawa, Y. Katayama, T. Miura, J. Electrochem. Soc. 154 (2007) F211.